

**HYDROPHOBIC
POLYTETRAFLUOROETHYLENE (PTFE)
COATING ON ENDOSCOPIC LENSES VIA RF
MAGNETRON SPUTTERING METHOD**

NABILAH BINTI SAUDI

UNIVERSITI SAINS MALAYSIA

2022

**SCHOOL OF MATERIALS AND MINERAL RESOURCES ENGINEERING
UNIVERSITI SAINS MALAYSIA**

**HYDROPHOBIC POLYTETRAFLUOROETHYLENE (PTFE) COATING ON
ENDOSCOPIC LENSES VIA RF MAGNETRON SPUTTERING METHOD**

**By
NABILAH BINTI SAUDI
Supervisor: Assoc. Prof. Dr. Yeoh Fei Yee**

Dissertation submitted in partial fulfillment of the requirements for the degree of
Bachelor of Engineering with Honour
(Materials Engineering)

Universiti Sains Malaysia

July 2022

DECLARATION

I hereby declare that I have conducted, completed the research work and written the dissertation entitled 'Hydrophobic Polytetrafluoroethylene (PTFE) Coating on Endoscopic Lenses via RF Magnetron Sputtering Method'. I also declare that it has not been previously submitted for the award of any degree and diploma or other similar title of this for any other examining body or University.

Name of student: Nabilah binti Saudi

Signature:

Date: 18/08/2022

Witness by

Supervisor: Associate Prof. Dr. Yeoh Fei Yee

Signature:

Date: 19/08/2022

ACKNOWLEDGEMENT

Bismillahirrahmanirrahim. First and foremost, praise Allah S.W.T as He gave me the strength to complete my final year project with ease. I would like to express my gratitude to the Dean of School of Materials and Mineral Resources Engineering Universiti Sains Malaysia, Prof. Ir. Dr. Mariatti Jaafar, and School of Materials and Mineral Resources Engineering, Universiti Sains Malaysia for providing the necessary resources, facilities, and materials to accomplish this project.

Furthermore, I would love to show my most sincere gratitude to my supervisor, Assoc. Prof. Dr. Yeoh Fei Yee, for his guidance, supervision, and continuous support for me during completing this project. Without him, I might be lost in doing progress in this project. All the advice and guidance given have been a great support for me to successfully completing and enjoy this project as part of my degree journey.

Moreover, I would like to extend my gratitude to the technicians and administration of School of Materials and Mineral Resources Engineering, USM, for their support and assistance in making the study a success.

Besides, I would like to thank my friends and individuals who have contributed to my work directly and indirectly. Thank you so much for your good deeds and enlighten all the time. May God ease your journey as well as your help in easing my journey. Not to forget to mention my special gratitude and thanks to my parents, Encik Hidayfah Che Anuwa and Puan Noor Azlinda Mohamed Nasaruddin for their endless support in every aspect including mentally, physically and financially. I am greatly indebted for their love and encouragement upon completing this project.

Finally, a massive appreciation for myself for never giving up in doing this project especially when days are not on our side. Thank you.

TABLE OF CONTENTS

DECLARATION.....	i
ACKNOWLEDGEMENT.....	ii
TABLE OF CONTENTS.....	iii
LIST OF TABLES.....	v
LIST OF FIGURES.....	vi
LIST OF SYMBOLS.....	ix
LIST OF ABBREVIATIONS.....	x
ABSTRAK.....	xi
ABSTRACT.....	xiii
CHAPTER 1 INTRODUCTION.....	1
1.1 General Introduction	1
1.2 Problem Statement	4
1.3 Research Objectives	5
1.4 Scope of Research.....	5
CHAPTER 2 LITERATURE REVIEW.....	7
2.1 Endoscopy	7
2.2 Materials for Endoscopic Lens	10
2.2.1 Acrylonitrile butadiene styrene (ABS)	15
2.2.2 Styrene acrylonitrile (SAN)	16
2.3 Hydrophobic properties	17
2.3.1 Models of Wettability.....	18
2.4 Coating material	21
2.4.1 Fluorinated polymers.....	21
2.4.2 Polytetrafluoroethylene (PTFE) or Teflon	23
2.5 Coating Process.....	24

2.5.1	RF Magnetron Sputtering Method.....	26
CHAPTER 3 METHODOLOGY.....		31
3.1	Introduction.....	31
3.2	Coating on Endoscopic Lens	33
3.2.1	Materials and Chemicals	33
3.2.2	Coating Process.....	33
3.2.2(a)	Preparation of the samples	33
3.2.2(b)	RF Magnetron Sputtering Coating	33
3.2.3	Effect of Sputtering Time	35
3.3	Characterization of Hydrophobic Coated Gastroscopy Lens	36
3.3.1	Water contact angle	36
3.3.2	UV-Visible (UV-Vis Spectroscopy)	38
3.3.3	Fourier Transform Infrared (FTIR) Spectroscopy	39
3.3.4	Atomic Force Microscopy (AFM).....	40
3.3.5	Scanning Electron Microscopy (SEM)	42
CHAPTER 4 RESULTS AND DISCUSSION.....		43
4.1	Introduction.....	43
4.2	Characterization of the Uncoated Samples	43
4.2.1	Hydrophobicity and Optical Properties	43
4.2.2	Surface Chemistry and Topography	44
4.3	Selection of Hydrophobic Coating on Endoscopic Lens	48
CHAPTER 5 CONCLUSION AND FUTURE RECOMMENDATIONS.....		69
5.1	Conclusion	69
5.2	Recommendations for Future Research	70
REFERENCES.....		71

LIST OF TABLES

Table 2.1: Types of endoscopes.....	8
Table 2.2: The comparison of commodity and engineering thermoplastics in medical device applications	13
Table 2.3: Properties of ABS and SAN.....	16
Table 2.4: Typical properties of fluorinated polymers	22
Table 3.1: Parameters for ABS samples.....	35
Table 3.2: Parameters for SAN samples.....	36
Table 3.3: Electromagnetic spectrum and molecular effects.....	40
Table 4.1: Roughness value of uncoated SAN and ABS.....	48
Table 4.2: Comparison of coated samples	53
Table 4.3: Roughness value of SAN and ABS samples	64

LIST OF FIGURES

Figure 1.1: External anatomy of an Olympus flexible video endoscope.....	1
Figure 2.1: Internal part of the human body	7
Figure 2.2: The classification of thermoplastics	12
Figure 2.3: Chemical structure of methacrylate acrylonitrile butadiene styrene (MABS)	15
Figure 2.4: Chemical structure of styrene acrylonitrile (SAN)	16
Figure 2.5: Contact angle of hydrophilic and hydrophobic surface.....	18
Figure 2.6: a) Wenzel's model and b) Cassie-Baxter's model.....	19
Figure 2.7: The measurements of water sliding angles (WSA) along both the longitudinal and transversal directions	20
Figure 2.8: Molecular structure of polytetrafluoroethylene (PTFE)	23
Figure 2.9: Schematic diagram of sputtering	27
Figure 2.10: Schematic diagram of magnetron sputtering system.....	28
Figure 3.1: Flowchart of the research methodology	32
Figure 3.2: Arrangement of samples on plate	34
Figure 3.3: The sputtering process was carried out at NOR lab in Physics school, USM Main Campus	34
Figure 3.4: Principles of advancing and receding contact angle measurements....	37
Figure 3.5: The symbolic representation of advancing and receding contact angle.	38
Figure 3.6: The electromagnetic spectrum	38
Figure 3.7: Schematic of the essentials of AFM	41
Figure 4.1: Contact angle of uncoated SAN and ABS	44
Figure 4.2: Contact angle images of uncoated (a) ABS and (b) SAN	44
Figure 4.3: Fourier transform infrared spectra of uncoated SAN and ABS	46

Figure 4.4: SEM images at uncoated ABS at (a) 100x and (b) 1000x magnifications	46
Figure 4.5: SEM images at uncoated SAN at (a) 100x and (b) 1000x magnifications	47
Figure 4.6: Atomic force microscopy of uncoated ABS at (a) phase contrast and (b) 3D image.....	47
Figure 4.7: Atomic force microscopy of uncoated SAN at (a) phase contrast and (b) 3D image.....	48
Figure 4.8: Bar chart of water contact angle of ABS coated-samples with different sputtering time	49
Figure 4.9: Water contact angle images of ABS coated-samples with sputtering time of (a) 30 minutes, (b) 60 minutes, (c) 90 minutes, and (d) 120 minutes.....	49
Figure 4.10: Bar chart of water contact angle of SAN coated-samples with different sputtering time	50
Figure 4.11: Water contact angle images of SAN coated-samples with sputtering time of (a) 30 minutes, (b) 60 minutes, (c) 90 minutes, and (d) 120 minutes.....	51
Figure 4.12: UV-Vis spectra (300-800nm) of ABS coated-samples	52
Figure 4.13: UV-Vis spectra (300-800nm) of SAN coated-samples	52
Figure 4.14: Transmittance against water contact angle for coated-samples	54
Figure 4.15: Fourier transform infrared spectra of SAN coated samples with different sputtering time	56
Figure 4.17: Fourier transform infrared spectra of ABS coated samples with different sputtering time	58
Figure 4.18: Fourier transform infrared spectra of ABS coated samples at sputtering time of a) 30 minutes, b) 60 minutes, c) 90 minutes and d) 120 minutes	59
Figure 4.19: Atomic force microscopy of 30 minutes sputtering time for coated-ABS (a) phase contrast and (b) 3D image.....	61

Figure 4.20: Atomic force microscopy of 60 minutes sputtering time for coated-ABS (a) phase contrast and (b) 3D image.....	61
Figure 4.21: Atomic force microscopy of 90 minutes sputtering time for coated-ABS (a) phase contrast and (b) 3D image.....	61
Figure 4.22: Atomic force microscopy of 120 minutes sputtering time for coated-ABS (a) phase contrast and (b) 3D image.....	62
Figure 4.23: Atomic force microscopy of 30 minutes sputtering time for coated-SAN (a) phase contrast and (b) 3D images	63
Figure 4.24: Atomic force microscopy of 60 minutes sputtering time for coated-SAN (a) phase contrast and (b) 3D image	63
Figure 4.25: Atomic force microscopy of 90 minutes sputtering time for coated-SAN (a) phase contrast and (b) 3D image	63
Figure 4.26: Atomic force microscopy of 120 minutes sputtering time for coated-SAN (a) phase contrast and (b) 3D image	64
Figure 4.27: SEM images of 30 minutes sputtering time for coated-ABS at (a) 100x and (b) 1000x magnifications.	65
Figure 4.28: SEM images of 60 minutes sputtering time for coated-ABS at (a) 100x and (b) 1000x magnifications.	65
Figure 4.29: SEM images of 90 minutes sputtering time for coated-ABS at (a) 100x and (b) 1000x magnifications.	66
Figure 4.30: SEM images of 120 minutes sputtering time for coated-ABS at (a) 100x and (b) 1000x magnifications.	66
Figure 4.31: SEM images of 30 minutes sputtering time for coated-SAN at (a) 100x and (b) 1000x magnifications.	67
Figure 4.32: SEM images of 60 minutes sputtering time for coated-SAN at (a) 100x and (b) 1000x magnifications.	67
Figure 4.33: SEM images of 90 minutes sputtering time for coated-SAN at (a) 100x and (b) 1000x magnifications.	68
Figure 4.34: SEM images of 120 minutes sputtering time for coated-SAN at (a) 100x and (b) 1000x magnifications.	68

LIST OF SYMBOLS

%	Percentage
°	Degree
μL	Microliter
nm	nanometer
sccm	Standard cubic centimeter

LIST OF ABBREVIATIONS

ABS	Acrylonitrile butadiene styrene
AFM	Atomic force microscopy
CAH	Contact Angle Hysteresis
CB	Cassie-Batter
ETFE	Ethylene-tetrafluoroethylene
FTIR	Fourier transform infrared spectroscopy
HA	Hydroxyapatite
HEA	High-Entropy Alloys
GI	Gastrointestinal
IBAD	Ion Beam Assisted Deposition
IPA	Isopropyl alcohol
MABS	Methacrylate acrylonitrile butadiene styrene
OR	Operating Room
PTFE	Polytetrafluoroethylene
RF	Radio Frequency
RMS	Root mean square
SAN	Styrene acrylonitrile
SEM	Scanning electron microscopy
UV-Vis	Ultraviolet-Visible
WCA	Water Contact Angle
WSA	Water Sliding Angle
ZnO	Zinc Oxide

**PELAPISAN HIDROFOBİK POLITETRAFLUOROETILENA (PTFE) PADA
KANTA ENDOSKOPIK MELALUI KAEDAH PERCIKAN MAGNETRON
FREKUENSI RADIO (RF)**

ABSTRAK

Endoskop digunakan sebagai alat untuk melihat bahagian dalaman tubuh manusia dalam peranti perubatan canggih terutamanya untuk pemeriksaan visual. Namun, masalah yang mengganggu prosedur ini adalah kemungkinan besar cecair badan manusia melekat pada kanta akan memberi had kepada pakar bedah untuk melihat bahagian yang dikehendaki di dalam tubuh manusia. Politetrafluoroetilena (PTFE) ialah salutan hidrofobik popular yang digunakan untuk menghalang bendalir daripada melekat pada kanta endoskop dan membantu dalam mengurangkan masa yang memakan masa untuk membersihkan permukaan kanta. Dalam kajian ini, kaedah percikan Magnetron Frekuensi Radio (RF) telah dilakukan untuk menyalut permukaan hidrofobik PTFE pada dua bahan kanta yang berbeza, iaitu akrilonitril butadiena stirena (ABS), dan stirena akrilonitril (SAN). Sifat fizikokimia sampel tidak bersalut dan bersalut PTFE dianalisis dengan menggunakan ujian sudut sentuhan air (goniometer), spektrometer UV-Vis, spektroskop Fourier-transform inframerah (FTIR), mikroskop elektron pengimbasan (SEM), dan mikroskop daya atom (AFM). Dalam projek ini, parameter yang disiasat adalah kadar sudut sentuhan air pada permukaan sampel pada masa percikan yang berbeza iaitu masa percikan 30 minit, 60 minit, 90 minit dan 120 minit. Berdasarkan keputusan SEM dan AFM, PTFE tidak merebak secara homogen ke atas permukaan sampel di mana ia mudah menyebabkan salutan terkeluar dari permukaan. Nilai kekasaran RMS sampel bersalut untuk kedua-

dua ABS dan SAN menunjukkan nilai peningkatan setiap masa percikan. Nilai-nilai RMS bagi sampel SAN adalah 50.7443 nm, 65.8518 nm, 74.1561 nm dan 78.9618 nm, bagi setiap masa percikan pada 30 minit, 60 minit, 90 minit, dan 120 minit. Manakala bagi sampel ABS adalah 15.1248 nm, 69.4297 nm, 66.0436 nm dan 72.0760 nm, bagi setiap masa percikan pada 30 minit, 60 minit, 90 minit, dan 120 minit. Di akhir projek ini didapati sampel terbaik dalam projek ini ialah SAN pada masa percikan 60 minit dengan penghantaran cahaya 98.29% dan sudut sentuhan 121.53° dan ABS pada masa percikan 60 minit dengan penghantaran cahaya 98.63% dan sudut sentuhan 94.28° .

HYDROPHOBIC POLYTETRAFLUOROETHYLENE (PTFE) COATING ON ENDOSCOPIC LENSES VIA RF MAGNETRON SPUTTERING METHOD

ABSTRACT

Endoscope was used as tool to view internal part of human body in advanced medical devices especially for visual examination. However, the problem that disrupt this procedure is high possibility of human body fluids to stick and attach on the lenses will give limitation to the surgeons to see the desired part inside human body. Polytetrafluoroethylene (PTFE) is a popular hydrophobic coating that used to prevent fluid from adhering on endoscope lens and helps in decreasing the time-consuming to clean up the surface of the lens. In this study, a RF Magnetron sputtering method was performed to coat PTFE hydrophobic surfaces on two different lens materials, which are acrylonitrile butadiene styrene (ABS), styrene acrylonitrile (SAN). Physicochemical properties of uncoated and PTFE-coated samples were analyzed by using water contact angle test (goniometer), UV-Vis spectrometer, Fourier-transform infrared (FTIR) spectroscope, scanning electron microscope (SEM), and atomic force microscope (AFM). In this study, the parameter that has been investigated was the water contact angle on the surface of the samples with different sputtering time, which were 30 minutes, 60 minutes, 90 minutes and 120 minutes. From this study, the best sample of SAN samples was during sputtering time of 60 minutes with transmittance of 98.29% and contact angle of 121.53°. Meanwhile, for ABS samples, the best sample of ABS was also during sputtering time of 60 minutes with transmittance of 98.63% and contact angle of 94.28°.

Based on the SEM and AFM results, PTFE does not spread homogeneously over the surface of samples where it is easily cause the coating to chip out from the surfaces. RMS roughness value of the coated-samples for both ABS and SAN show increase value each sputtering time. The RMS values for SAN samples were 50.7443 nm, 65.8518 nm, 74.1561 nm dan 78.9618 nm, for sputtering time of 30 minutes, 60 minutes, 90 minutes and 120 minutes, respectively. Whereas, the RMS values for ABS samples were 15.1248 nm, 69.4297 nm, 66.0436 nm dan 72.0760 nm, for sputtering time of 30 minutes, 60 minutes, 90 minutes and 120 minutes, respectively. For SAN samples, the best sample of SAN was during sputtering time of 60 minutes with transmittance of 98.29% and contact angle of 121.53°. Meanwhile, for ABS samples, the best sample of ABS was also during sputtering time of 60 minutes with transmittance of 98.63% and contact angle of 94.28°.

CHAPTER 1

INTRODUCTION

1.1 General Introduction

During laparoscopic surgery, it is very crucial to allow a surgeon to see clear visualization of the inside part of the patient's body which is inside of the abdomen (tummy) and pelvis without creating a large incisions in the skin. In order to undergo this process, the camera lens of an endoscopic are used to explore the internal body parts of the patients, are specifically for medical purposes in order to get details information about the causes of patients' health problems or sickness. However, during laparoscopic surgery, the endoscopic lens will covered by the body fluids and this might distract surgeons to see the path inside the patient's body. At the same time, surgeons will also face a hard time getting a good result from the surgery. Figure 1.1 showed the hand piece, insertion tube, and umbilical cord, which were the three primary parts of a standard gastrointestinal endoscope.

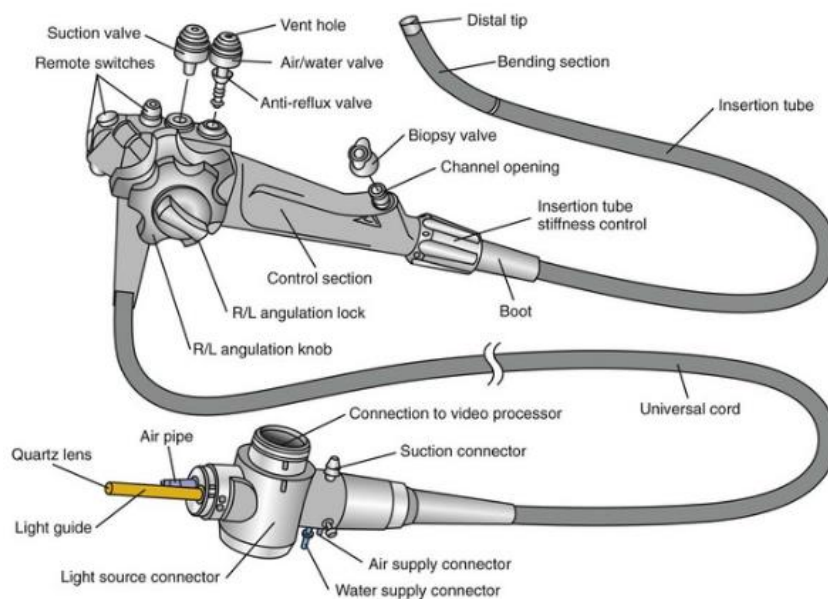


Figure 1.1: External anatomy of an Olympus flexible video endoscope

Endoscopes provide medical professionals with a window into the human body, although the image is frequently not very clear. It is necessary to regularly interrupt during operations to clean the lens end of the endoscope since blood and other biological fluids are sticky and clog up the viewing window. In addition to delaying the operating room (OR) staff's ability to clear the scope each time it becomes fouled, this consumes costly time and may interfere with a procedure's natural flow.

For achieving an adequate result from the surgery, surgeons need to keep on cleaning the lens that leads to an increase in the time consuming of the surgery. In order to prevent and minimize the inefficient time consuming to sterile the surface of the lens, the endoscopic lens are coated with coating material that have the property of hydrophobic as in human body, the total water varies from 45% to 75% of body weight (Khudhair, 2021). By meaning, there is high possibility for the endoscopic lens to cover by body fluid during its application in surgery. Therefore, there are several researcher that study the hydrophobic coating on endoscopic lenses in order to achieve optical surface cleanliness as well as retains a precise vision of the accessible area of the internal body part of the patients and to ease the endoscopy medical operation without any interruption.

In the past, the self-cleaning property of the superhydrophobic PTFE surface was investigated using aqueous methylene blue dye and activated carbon powder, where the aqueous dye easily wetted the untreated glass surface, whereas the superhydrophobic PTFE surface remained dry and stain-free. As a contaminant example, activated carbon powder was dispersed on both the tilted superhydrophobic surface and the untreated glass surface, and water droplets were continuously dropped onto the two surfaces. As a result, droplets of water effectively picked up carbon powder and rolled away from the superhydrophobic PTFE surface, achieving the self-

cleaning performance. On the untreated glass surface, however, some carbon powder remained. This 'Lotus effect' has a lot of potential for dirt-resistant self-cleaning applications (Zhuang et al., 2017).

The optical, structural, and morphological properties of thin and ultrathin Polytetrafluoroethylene (PTFE) sputtered films as a function of deposition time. It was discovered that all of the samples have a contact angle close to 100, indicating that the deposited films are hydrophobic. The presence of CF_3 radicals, in addition to CF_2 radicals discovered during FTIR characterization in the RF sputtered PTFE films, contributes to a decrease in surface energy, making the films hydrophobic (Tripathi et al., 2016).

Magnetron sputtering is an easy way to create nitride-based high-entropy alloys (HEA) coatings. The primary factors that determine coating qualities are target composition, bias voltage, and gas flow rate. Magnetron sputtering HEA coatings have exceptional qualities such as hardness and Young's modulus, corrosion and wear resistance, thermal stability at high temperatures, and diffusion retardation. HEA coatings have demonstrated exceptional wear resistance and can be utilised to extend the life of orthopaedic implants. (Padamata et al., 2022)

Hariharan et al. (2020) reported that RF magnetron sputtering effectively deposits TiN/AISI 1018 coating. TiN layers were sprayed by RF Titan in a N_2 atmosphere in this article. Micro hardness and adhesion were assessed in heat-treated layers deposited on low carbon metal under varied environmental conditions. Changes in form and morphology were seen throughout various heat treatments. RF magnetron sputtering effectively generated C-TiN staining.

Furthermore, the desire for coatings with increased functional qualities and the deposition of non-metallic/non-conductive thin films prompted the development of

innovative magnetron sputtering ideas. High-power pulsed magnetron sputtering, dual-magnetron sputtering, and radio frequency (RF) magnetron sputtering of non-conductive objects are among them. In terms of the latter, RF magnetron sputtering was shown to be ideal not only for the synthesis of inorganic materials (e.g., glasses, metal oxides, and nitrides), but also for the deposition of polymer-like coatings, or plasma polymers (Kylíán et al., 2019). In comparison to normal polymers, such materials exhibit significantly greater degrees of cross-linking and branching, as well as the absence of regularly recurring monomer units. Despite their random and inherently complex structure, plasma polymers appear to be a highly valuable class of materials for a variety of applications, including dielectric separation layers, permeation barriers or gas separation membranes, laser facilities, adhesion-promoting coating, and films that allow fine-tuning of surface wettability and bio-adhesive/bio-repellent behavior (Macgregor and Vasilev, 2019)

1.2 Problem Statement

Endoscopic lens are widely used as medical devices in examining and identifying patients' problem in the internal part of their body that hardly can be view by technology such as X-ray. As endoscopic lens are required to identify the implication inside of the gastrointestinal tract of the patient, there are high possibility to have lens attached and covered with body fluids such as tissues, mucus and acid. These substances will block the view of the track inside patients' body and give hard time to surgeon to detect any problems in the internal part of their body. The properties of coating material should include hydrophobicity, transparency, conformability, mechanical adhesion, and biocompatibility. In order to minimize this problem, the coating material used is PTFE via RF magnetron sputtering method.

In order to improve the hydrophobicity of the surface, various parameters are required to control through the coating process. Sputtering factors including substrate temperature, deposition rate, substrate-target distance, gas pressure, and RF power all have an impact on the structural, electrical, and optical characteristics of ZnO films. The microstructure of the film or its quality, which comprises surface roughness, adhesion, impurity, and density, is the outcome of the interaction of the above characteristics. When such parameters are appropriately tuned, they allow a high degree of control over the film growing process. As a result, in order to develop high-quality products, the following aspects must be under control. Therefore, the optimization of deposition rate, sputtering distance, gas flow ratio, working pressure and power for depositing film at moderate temperature by RF magnetron sputtering method (Muthukarappan et al., 2019).

1.3 Research Objectives

This research is aim to determine the suitability of materials coating to provide the properties of hydrophobicity on the endoscopic lens. The research objectives of this project are:

1. To estimate the hydrophobic of polytetrafluoroethylene (PTFE) coating on endoscopic lenses via RF magnetron sputtering method with different sputtering time duration
2. To characterize the physicochemical properties of the coated lenses

1.4 Scope of Research

In this study, the surface of the lenses are coating with polytetrafluoroethylene (PTFE) via RF magnetron sputtering method, one of the method in physical vapor

deposition (PVD). PTFE used as a coating material to refine the hydrophobic property on the endoscopic lens during the lens application especially in medical surgery. The sputtering time of coating process determined the efficacy of hydrophobic level for PTFE on the endoscopic lens.

Several method of characterization determined the effectiveness of the PTFE as the hydrophobic coating on the surface of the samples prepared (uncoated and coated samples). The hydrophobic of the coated samples measured by using a goniometer where it gave the water contact angle when liquid put on the samples. Next, the light transmittance of the samples observed by using the ultraviolet-visible light (UV-Vis) spectroscopy. Moreover, the functional groups that existed on the samples detected by using the Fourier transform infrared (FTIR) spectroscopy. Lastly, the surface morphology and topography of the samples inspected by using scanning electron microscopy (SEM) and atomic force microscopy (AFM).

CHAPTER 2

LITERATURE REVIEW

2.1 Endoscopy

Endoscopy is a medical procedure where a tiny instrument commonly a tube-like tool known as an endoscope. Endoscopic surgery, which created in response to the growing demand for less invasive treatment, is now quickly broadening its applications in variety of surgical specialties, including urology, obstetrics/gynecology, respiratory surgery, endocrine surgery, paediatric surgery, orthopaedic surgery and anesthesiology. Endoscopes are flexible instruments which is a combination of fiber-optics (for illumination) and charge-coupled devices (for imaging) that are used as a medical device to examine the internal part of the human body (Kohli and Baillie, 2019). Figure 2.1 showed the common internal part of human body that required endoscopy in order to identify sickness or abnormal condition of the patient.

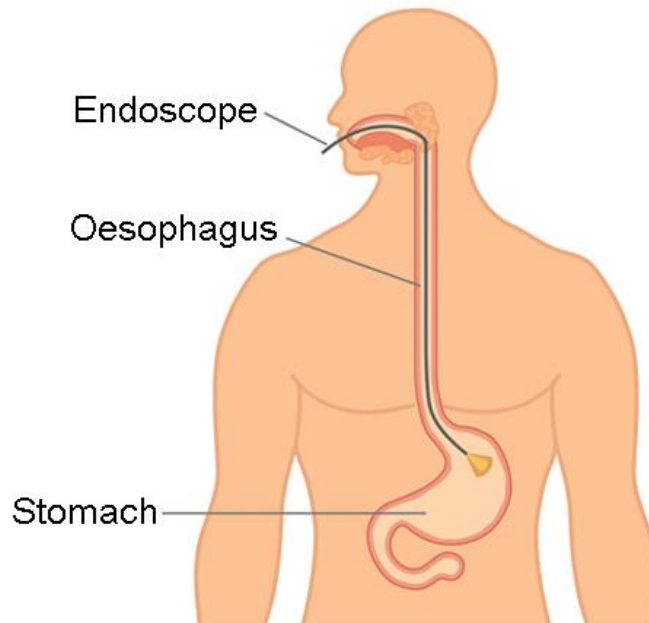


Figure 2.1: Internal part of the human body

Endoscopes commonly used in identifying the pathological state of the patient especially in the gastrointestinal (GI) tract, the bronchial system, the ureters, and other body cavities. There are many types of endoscopes available on market depending on which part of the interior of inaccessible sites in patient's body. According to Cancer.net Editorial Board, there are multiple types of endoscopes as shown in Table 2.1.

Table 2.1: Types of endoscopes (Cancer.Net Editorial Board, 2019)

Name of procedure	Name of tool	Area or organ viewed	How endoscope reaches target area
Anoscopy	Anoscope	Anus and/or rectum	Inserted through the anus
Arthroscopy	Arthroscope	Joints	Inserted through a small incision over the joint
Bronchoscopy	Bronchoscope	Trachea, or windpipe, and the lungs	Inserted through the mouth
Colonoscopy	Colonoscope	Entire length of the colon and large intestine	Inserted through the anus
Colposcopy	Colposcope	Vagina and cervix	Placed at the vagina's opening after a tool called a speculum dilates the vagina. It is not insert in the body.

Cystoscopy	Cystoscope	Inside of the bladder	Inserted through the urethra
Esophagoscopy	Esophagoscope	Esophagus	Inserted through the mouth
Gastrosocopy	Gastroscope	Stomach and duodenum, which is the beginning of the small intestine	Inserted through the mouth
Laparoscopy	Laparoscope	Stomach, liver, or other abdominal organs, including female reproductive organs, including the uterus, ovaries, and fallopian tubes	Inserted through a small, surgical opening in the abdomen
Laryngoscopy	Laryngoscope	Larynx, or voice box	Inserted through the mouth
Neuroendoscopy	Neuroendoscope	Areas of the brain	Inserted through a small incision in the skull
Proctoscopy	Proctoscope	Rectum and sigmoid colon, which is the bottom part of the colon	Inserted through the anus
Sigmoidoscopy	Sigmoidoscope	Sigmoid colon	Inserted through the anus

Thoracoscopy	Thoracoscope	Pleura, which are the 2 membranes covering the lungs and lining the chest cavity, and structures covering the heart	Inserted through a small surgical opening in chest
--------------	--------------	---	--

Scandinavian nations have been at the forefront of research comparing laparoscopic versus open cholecystectomy (Hendolin and Pääkönen, 2000). Both of these studies reach the same conclusions: laparoscopic surgery significantly reduced postoperative pain, reduced respiratory insufficiency, and decreased hospital stay and work-off periods when compared to open surgery, while there were no changes in the indicators of surgical invasion, such as blood CRP, IL6, urine adrenalin, and cortisol levels.

In addition, even though laparoscopic surgery for appendicitis takes longer than open surgery, the risk of complications is similar, and numerous studies concur that the advantages of less invasive laparoscopic surgery include a reduced risk of wound infection, reduced postoperative pain, a shorter hospital stay, and quicker recovery (Taginawa, 2009)

2.2 Materials for Endoscopic Lens

The materials of the endoscopic lens are selected based on the capability of the materials to endure the condition inside the human body as the endoscopic lens will be going through inside the internal part of the patient's body. As the lens will be covered with the body fluids during the surgery, the desirable properties of the lens material have to achieve in order to get a clear view of the camera when entering the path of the body.

The usage of plastics are widely utilized in the industry, especially in manufacturing parts for medical devices which are approximately 5-7 million metric tons of plastic, which is about 1-2% of the global plastics production. One of the reasons for the expansion of plastics used in medical device applications is the demand for new technologies, such as diagnostic imaging, laser surgery, implants, and endoscopy surgery, which required polymers to improve their biocompatibility properties. In accordance with Sastri (2010), commodity plastics account for about 80% of plastics used for medical devices in applications such as lab ware, containers, and molded connectors. Meanwhile, engineering plastics stated a higher rate of growth as consequence of the need for materials in surgical, drug delivery, self-treatment, preventative medicine, and diagnostic testing.

As shown in Figure 2.2 below, there are two categories of thermoplastics; amorphous and semi-crystalline polymers. Amorphous is where the polymer chains are randomly oriented and lack order. This condition leads to the influence of the density of loops and bends towards the mechanical properties and the temperature-dependent chain mobility. Below the glass transition temperature T_g , the chains are frozen and unable to move with ease which leads to producing brittle materials. On the other hand, above T_g , the chains are mobile and able to rearrange to accommodate mechanical deformation as the material can be stretched (Frick et. al., 2019).

Semi-crystalline thermoplastics are polymer chains that are moderately order as the chains will align themselves with each other restrictedly upon cooling from the melt, which will form small crystalline regions. Semi-crystalline polymers generally have much higher ductility compared to amorphous polymers as amorphous produced brittle materials. While semi crystalline has improved toughness, resistance to crazing

and stress cracking, and is less susceptible to chemical or environmental attack (Frick et. al., 2019)

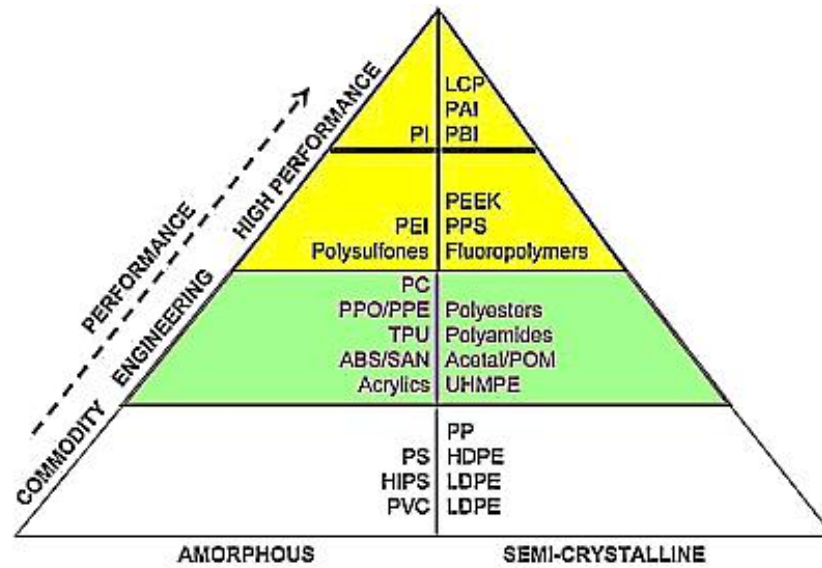


Figure 2.2: The classification of thermoplastics

Table 2.2: The comparison of commodity and engineering thermoplastics in medical device applications (Sastri, 2010)

Property	Commodity Plastics	Engineering Thermoplastics
Heat deflection temperature under 4.6 kgf/cm ² (66 psi)	70-150°C (158-302 °F)	125-280 °C (257-536 °F)
Continuous use temperature	45-80 °C (113-176 °F)	90-250 °C (194-482 °F)
Tensile strength	150-1000 kgf/cm ² (2100-4100 psi)	600-2500 kgf/cm ² (8500-35500 psi)
Flexural modulus	1.0-5.0 kgf/cm ² ×10 ⁴ (14-70 psi ×10 ⁴)	2.5-12.0 kgf/cm ² ×10 ⁴ (35-170 psi ×10 ⁴)
Compressive strength	3.0-11.0 kgf/cm ² ×10 ⁴ (42-156 psi ×10 ⁴)	8.0-11.0 kgf/cm ² ×10 ⁴ (113-156 psi ×10 ⁴)
Medical device applications	<ul style="list-style-type: none"> • Tubing • Films, packaging • Connectors • Lab ware • Drug-delivery components 	<ul style="list-style-type: none"> • Surgical instruments • Blood set components • Implants • Dental instruments • Surgical trays

Examples of plastics	<ul style="list-style-type: none"> • PS • HIPS • PVC • PP • HDPE • LDPE 	<ul style="list-style-type: none"> • PC • PPO/PPE • TPU • ABS/SAN • Acrylics • Polyesters • Polyamides • Acetal/POM • UHMPE
----------------------	---	--

According to the research paper of Kim, Chang and Kwon (2021), the other materials that can be used for endoscopic lenses are APL5014CL (Cyclo-Olefin Copolymer, COC) and OKP-A2. APL5014CL is a Cyclo-Olefin Copolymer (COC) material with properties such as refractive number of 1.54 and an Abbe number of 56.0. It has a crown-like plastic material that is acceptable for the lens' manufacture as it has low water absorption, low autofluorescence, high chemical resistance and high refractive index. Meanwhile, OKP is a special polyester material from coal chemistry that is commonly used in optical industry. The OKP products are known for their high purity optically clear thermoplastic with high performance optical components such as phone and camera lenses. OKP-A2 has a refractive index of 1.66 and an Abbe number of 20.4. Moreover, comparing these two materials, OKP-A2 has higher dispersion than APL5014CL.

Huang et al. (2022) reported that the use of liquid crystal (LC) lenses are active optical components where they contain electrically tunable focal lengths without any instinctive movements. The high-resistive layer for LC lens illustrated low operating voltage, fast response time and high optical performance.

In this project, ABS and SAN were chosen to be the materials of the substrate or samples as these materials are widely used in medical devices and easy to find the suppliers that can provide it.

2.2.1 Acrylonitrile butadiene styrene (ABS)

Acrylonitrile butadiene styrene (ABS) is one of the important thermoplastic and amorphous polymer that has been well known for its resistance to impact. ABS contains three monomers, which are acrylonitrile, butadiene, and styrene. From these combinations, it is able to provide beneficial physical properties such as high rigidity, good impact resistance even at low temperatures, good insulating properties, good weldability, and abrasion and strain resistance (Ziabka et. al., 2020).

The transparent version of ABS is known as methacrylate acrylonitrile butadiene styrene (MABS) which has similar thermal and mechanical properties to ABS. The transparency is attained by matching the refractive indices of the matrix resin (the transparent acrylate-acrylonitrile-styrene polymer) with polybutadiene rubber impact modifier (Sastri, 2010).

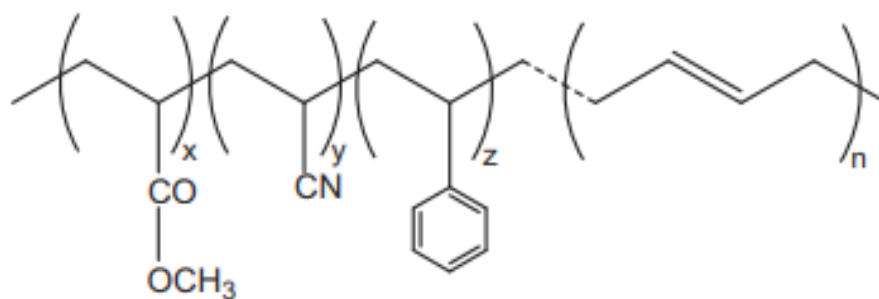


Figure 2.3: Chemical structure of methacrylate acrylonitrile butadiene styrene (MABS)

2.2.2 Styrene acrylonitrile (SAN)

The copolymerization of acrylonitrile with styrene helps in enhancing the heat and chemical resistance compared to styrene. The properties in SAN include high transparency, high gloss and maintains its gloss even at low temperatures (Sastri, 2010). Styrene-based materials provide distinctive characteristics of durability, high performance, versatility of design, simplicity of production and economy.

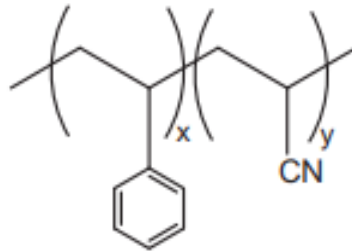


Figure 2.4: Chemical structure of styrene acrylonitrile (SAN)

Table 2.3: Properties of ABS and SAN (Sastri, 2010)

Property	Units	MABS	SAN
Density	g/cc	1.08	1.08
Transmission (visible)	%	90	87-95
Water absorption, 24 h	%	0.7	0.25
Glass transition temperature	°C	100-105	110
HDT at 0.46 MPa or 66 psi	°C	90-100	95-110
HDT at .8 MPa or 264 psi	°C	75-90	80-90
Softening point	°C	91	97
Tensile strength at break	MPa	35-45	30-50
Elongation at break	%	10-20	7-20

2.3 Hydrophobic properties

Interactions of hydrophobic are not precisely happen due to bonding, so there is no such thing as a hydrophobic bond. The interactions are interfacial phenomena that happened due to the net effects of attractive and repulsive forces that formed between solid surfaces, dissolved hydrocarbons, and highly polar solvents. Wettability of a material's surface shows how fluids interact with such surfaces as wetting behavior is universal but varies in a peculiar nature. The nearest examples of wettability is from plants such lotus leaf. Lotus leaves known for their property of 'never wetting' or 'ultra-ever dry' which water can roll on the lotus leaf's surface freely, at point where the droplets of water can see clearly. The water droplets demonstrate almost spherical shape enabling the rolling behavior. This behavior invented a self-cleaning property because contaminants can removed by the rolling drop (Barthlott and Neinhuis, 1997). In addition, the identical behaviour can observed in rice leaves as well. It display anisotropic non-wetting state as it enables water rolls easily due to the longitudinal directional instead of the perpendicular direction on the surface (Wu et. al., 2011).

Liquids have a natural tendency to attach to objects, including themselves. As a result, the way a surface interacts with liquid, specifically water droplets, determines whether it is hydrophobic (fearful of water) or hydrophilic (attract to water). A droplet that makes no contact with a surface forms a perfect spherical and has a contact angle of 180° , whereas a water droplet that thoroughly wets the surface has a contact angle of 0° . (Zhang and Xu, 2018) The condensation of water vapor on a solid surface can occur in two different ways which are dripping and film-like condensation. In droplet condensation, when water vapor condenses on a low-energy surface, it forms a myriad of small water droplets with large contact angles. In this case, the effects of cloudiness

will appear even if the surface is not completely wet. However, it must be condensed on a high energy substrate as water droplets on the surface show a very low contact angle (that is, condensation per film). Here, no fogging is observed because a thin film of water is formed on the surface and does not significantly impede the transmission of light. (Duran and Laroche, 2018)

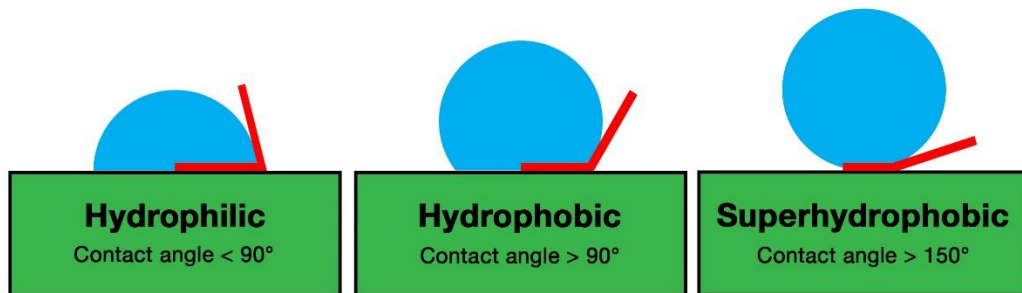


Figure 2.5: Contact angle of hydrophilic and hydrophobic surface

2.3.1 Models of Wettability

In a normal daily routine as a human, various wetting phenomenon can be notice. For instance, raindrops on lotus leaves and droplets of cold water on glasses. In the occurrence of wetting, there are two aspects of it, which are static wetting and dynamic wetting. In this project, the mainly aspects that will be focused on is static wetting as it is mainly deliberated in terms of hydrophobicity, water contact angle, wetting of structured surface in Wenzel state and Cassie-Baxter state (CB state). These two phenomenon also known for their thermodynamic equilibrium contact angle on rough and heterogenous surfaces.

The condition where the micro and nano structures on the surface can enhance the wetting property of the solid surface as proven by Wenzel in Figure 2.6 a). Wenzel pointed rough surface and specified it by a roughness ratio factor. Moreover, the roughness is one of the factor that helps in improving the surface's wetting property

that can be measured in two ways. One, when the liquid was initially wetting on a flat and smooth surface, it can enhance the hydrophilicity whereas if the liquid was non-wetting on a flat surface, it will give an improvement of hydrophobicity (Banerjee, 2008).

On the other side, a hydrophobic surface can be prove when a droplet of liquid can easily slides down from the surface as there are air pockets forming between the droplet and the structure on the surface. The droplet forms a phenomenon known as Cassie-Baxter (CB) wetting state as shown in Figure 2.6 b) and therefore, the effective surface tension between the liquid and the textured surface becomes lower than that of the flat surface (Kim and Ryu, 2020). According to Yuan and Lee, (2013), Wenzel and Cassie-Baxter's angles are not equivalent to Young's contact angle as the Young equation results from the equilibrium of forces acting on the triple line.

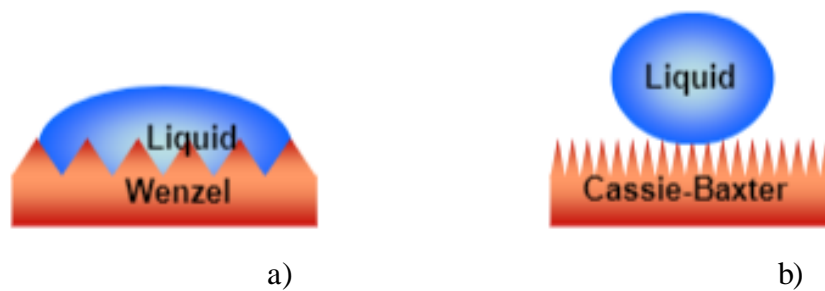


Figure 2.6: a) Wenzel's model and b) Cassie-Baxter's model

A low water adhesion can be clarified by the heterogeneous wetting theory proposed by Cassie. According to Cassie's approach, the trapped air will leading to the inadequate of the liquid to wet the surface alleys. This is why the grooves and peaks in the surface profile are in contact with the air and the liquid, respectively (Khaskhoussi et al., 2021).

Figure 2.6 below displayed the measurements of water sliding angles (WSA) along both the longitudinal and transversal directions. Khaskhoussi et al. (2021)

explained that the figure below showed that Al-WS surface reached a WSA $>90^\circ$, which was a typical of the pure Wenzel state. In contrast, the Al-FS surface achieved a very low WSA, which almost reach to zero that known as typical of a pure Cassie–Baxter state. Meanwhile, an intermediate behaviour was determined for the Al-NS surface.

As observed from the respective figure, there was the lowest sliding angles in the opposite direction of the lamination (transverse). These findings are consistent with the roughness analysis. Indeed, the AFM analysis of the bidirectional profiles revealed that the transverse gap between the peaks and valleys was greater than the longitudinal gap, promoting water droplet rolling (Khaskhoussi et al., 2021). Pockets of air can be stably entrapped on the roughness profile in connection with the water/substrate interface in such a configuration, significantly reducing the contact area between the solid and the water droplet and allowing for easier water sliding due to the high effective combined action of the silane-induced hydrophobicity and micro-nano roughness.

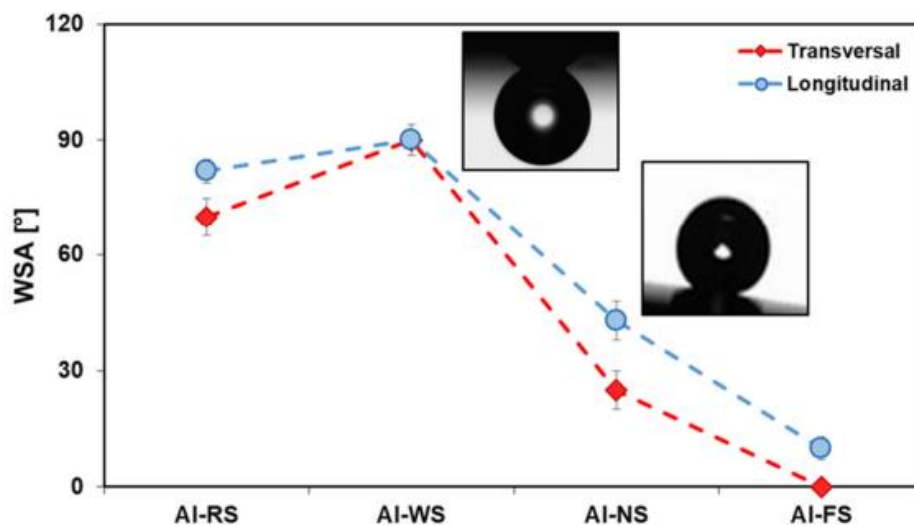


Figure 2.7: The measurements of water sliding angles (WSA) along both the longitudinal and transversal directions (Khaskhoussi et al., 2021)

2.4 Coating material

The properties of the chosen coating material are crucial to make sure it is suitable for the desirable properties of the final product. The process of choosing an appropriate coating material is a very important process as the device with the coated material will put in the human body. It is crucial to make sure that the coating is uniform, and completely covered every part of the surface at which usually contained a complex structure and diminishes the bringing across the structure.

Traditionally, materials and coatings with a contact angle between water and aqueous solutions greater than 90° were referred to be hydrophobic materials. Materials that are hydrophobic or superhydrophobic have a variety of special functional qualities, including the ability to repel water, resist corrosion, and be stable in the presence of biofouling, inorganic, and (in some circumstances) organic contaminants (Boinovich and Emelyanenko, 2008). Fluid flows very easily near the hydrophobic surfaces of such materials. A wide range of methods for creating the superhydrophobic condition of surfaces, which is required for textured surfaces, were put forth. The following are the methods that are currently most regularly utilized:

1. Nanoparticle and film electrodeposition and electrochemical deposition, followed by hydrophobic material treatment
2. Following by treatment with hydrophobic materials, organised structures are created by chemical vapour deposition
3. Etching of the surface of materials followed by treatment with hydrophobic materials.

2.4.1 Fluorinated polymers

Fluorinated polymers create a unique classification of materials with a combination of attractive properties as it formed by strong carbon-carbon bonds and

stable carbon-fluorine bonds. Moreover, the interesting properties are also present due to the special electronic structure of the fluorine element characterized by high electronegativity, low polarizability, and small van der Waals radius (1.32 Å) (Ebnesajjad, 2015). Due to those inherent characteristics, fluorinated polymers exhibit high thermal stability, weather stability, low coefficient of friction, and lower surface energy, especially taking non-fluorinated groups as an approach. In addition, fluorinated polymers are chemically stable and unreactive. As the fluorine induces higher stability compared to chloride, hence the reactivity will diminish with the rise of fluorine content. The typical properties of fluorinated polymers are shown in Table 2.4 below.

Table 2.4: Typical properties of fluorinated polymers (Vanessa F. Cardoso et. al., 2018)

Type of fluorinated polymers	Density (g. cm ⁻³)	Melting point (°C)	Refractive index
Polytetrafluoroethylene (PTFE)	2.16	327	1.35
Polyvinyl fluoride (PVF)	1.40	190	1.46
Polyvinylidene fluoride (PVDF)	1.75	170	1.42
Fluorinated ethylene propylene (FEP)	2.15	260	1.34
Perfluoroalkoxy (PFA)	2.15	310	1.34
Polyethylene tetrafluoroethylene (ETFE)	1.70	270	1.40
Polychlorotrifluoroethylene (PCTFE)	2.10	210	1.44

One of the attractive characteristics related to fluorinated polymers is their superwetting properties as they show the ability to develop microtextured surfaces due to the formation of a stable air-liquid interface, inducing special features on the material (Liu et. al., 2017). Therefore, the surfaces of superhydrophobic, superhydrophilic, superamphiphobic, and directional liquid-transfer can be achieved by adding the combination of wettability with adhesion or optical properties.

2.4.2 Polytetrafluoroethylene (PTFE) or Teflon

Polytetrafluoroethylene (PTFE) or also known as Teflon is a fluoropolymer which is polymerized from the monomer tetrafluoroethylene (TFE) as shown in Figure 2.6. It possesses the C-F bond in the PTFE formulation, which consists of the molecular formula $[(CF_2 - CF_2)_n]$. It is one of the well-known engineering material as it has an excellent physical and chemical properties that very useful in variety of application. It has an outstanding thermal stability and toughness at low temperature, low thermal conductivity, perfect insulating and dielectric properties, extremely low coefficient friction and chemical resistance. The composition and structure of PTFE are useful as protective layer or coating such as superhydrophobic composite coating (Wang, 2016).

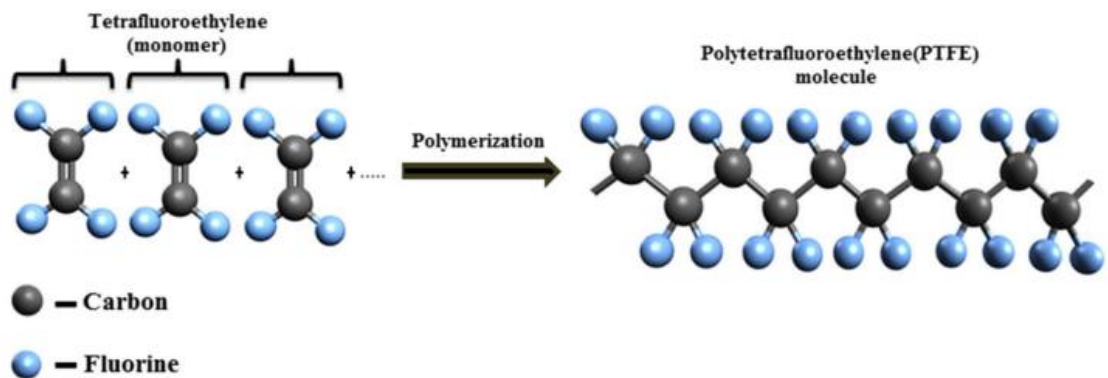


Figure 2.8: Molecular structure of polytetrafluoroethylene (PTFE) (Dhanumalayan and Joshi, 2018)

The interesting part of PTFE is PTFE products has the originality of repelling water, oil and adhesives, which suitable with the application of endoscope lens. PTFE exhibited superior hydrophobic nature due to its low surface energy. As stated by Naftalovich et. al., (2016), PTFE is proposed as a nonmetabolized food volume bulking agent for human ingestion. Moreover, PTFE proven as a safe in regards to immune toxicity, specifically for ingestion purposes. The study reported large volume ingestion of PTFE, at 25% of the diet, considered as safe based on extensive animal feeding trials and the extreme inertness of the material.

Given its structure, PTFE behaves generally like a non-polar polymer and is suitable for low-adhesion applications while having highly energetic and polarised links. Because of its mechanical resilience and chemical inertness, which prevent organic molecules from adhering to its surface, PTFE is one of the materials most frequently employed for decreasing contamination and improving hygiene (Rondinella et al., 2021)

The intensity of PTFE's diffraction peaks considerably rises with increasing PTFE addition. Furthermore, the contents of C and F on the coated surface rise with increased PTFE addition, indicating that PTFE deposition is rising. Based on their results of surface micro-nano morphology and wettability, it is clear that the surface morphology has changed, generating a rough surface with convex-like patterns adorned with PTFE nanoparticles. This rough surface has enough micro-nano structure to increase the hydrophobicity (Wang et al., 2020).

2.5 Coating Process

One of the surface coating techniques is vapor phase process deposition, which is divided into two types; chemical and physical vapor deposition. When the surface